Trends in
Biochemical Sciences

CellPress
OPEN ACCESS

Review

From algae to plants: understanding pyrenoid-based CO_2-concentrating mechanisms

Ella Catherall[1,2,4], Sabina Musial[3,4], Nicky Atkinson[1,2], Charlotte E. Walker[3], Luke C.M. Mackinder[3,*], and Alistair J. McCormick[1,2,*]

Pyrenoids are the key component of one of the most abundant biological CO_2 concentration mechanisms found in nature. Pyrenoid-based CO_2-concentrating mechanisms (pCCMs) are estimated to account for one third of global photosynthetic CO_2 capture. Our molecular understanding of how pyrenoids work is based largely on work in the green algae *Chlamydomonas reinhardtii*. Here, we review recent advances in our fundamental knowledge of the biogenesis, architecture, and function of pyrenoids in *Chlamydomonas* and ongoing engineering biology efforts to introduce a functional pCCM into chloroplasts of vascular plants, which, if successful, has the potential to enhance crop productivity and resilience to climate change.

Highlights

Pyrenoid-based CO_2-concentrating mechanisms (pCCMs) enhance CO_2 fixation in nearly all eukaryotic algae and some nonvascular plants (most hornwort species). The unicellular green alga *Chlamydomonas reinhardtii* has the most well-characterised pCCM.

The *Chlamydomonas* pyrenoid has three characteristic architectural features: a liquid-like ribulose-1,5-bisphosphate carboxylase/oxygenase (Rubisco) matrix, specialised tubular thylakoids called pyrenoid tubules, which traverse the matrix; and a sheath of starch plates that surround the matrix.

Recent work in *Chlamydomonas* and *in planta* has advanced our functional understanding of each of these architectural features, and the components and energetic requirements of CO_2 delivery to the pyrenoid.

Models predict that introducing a functional pCCM into plants could increase crop yield and resilience. Significant progress has now been made in engineering all three architectural features into plants.

An introduction to pyrenoids

Ribulose-1,5-bisphosphate carboxylase/oxygenase (Rubisco) catalyses net CO_2 capture in all photosynthetic organisms. However, Rubisco is limited by a relatively slow catalytic rate and catalyses an energetically wasteful competitive oxygenation reaction [1]. To compensate, almost all eukaryotic algae have evolved a specialised microcompartment called the pyrenoid, in which Rubisco is sequestered. The pyrenoid works with inorganic carbon delivery components of the p**CCM** (see Glossary) to improve photosynthetic CO_2 uptake by concentrating CO_2 near Rubisco, preferentially driving carboxylation over oxygenation. It is suggested that pyrenoids arose in algae after the evolution of plants in response to the high atmospheric O_2 and low CO_2 during the late Permian, which may explain the lack of pyrenoids in almost all plant lineages [2–4], with the exception of several species of hornwort bryophytes (i.e., nonvascular plants), where pyrenoids may have evolved more recently [5].

Our understanding of how pyrenoids assemble and function is based primarily on work in the model green alga *Chlamydomonas*, although very recent efforts are expanding into diatoms, hornworts, and other algae [6–11]. The availability of mutant libraries [12] and efficient fluorescent protein tagging [13] in *Chlamydomonas* has allowed researchers to characterise pCCM components *in vivo*, and subsequently reconstitute key elements of the pyrenoid architecture *in vitro* [14–16]. Many pCCM components appear readily transferable into model **C3 plants**, such as *Arabidopsis* and tobacco, which has helped accelerate efforts to assemble a functional pCCM into crops (for recent reviews, see [4,17]).

The *Chlamydomonas* pyrenoid is dynamic and can rapidly increase in size and complexity in response to low CO_2 conditions when the pCCM is active. The structural architecture of the pyrenoid has three characteristic features (Figure 1). First, the core of the pyrenoid comprises primarily Rubisco and the Rubisco-linker protein EPYC1, which phase-separate to form a liquid-like Rubisco matrix [18,19]. Second, the matrix is traversed by specialised **pyrenoid tubules**, which are continuous with the typical sheet-like thylakoid membranes in the surrounding chloroplast stroma [20]. How the pyrenoid tubules form remains unclear, but they assemble into a complex network and

[1]Institute of Molecular Plant Sciences, School of Biological Sciences, University of Edinburgh, Edinburgh, EH9 3BF, UK
[2]Centre for Engineering Biology, University of Edinburgh, Edinburgh, EH9 3BF, UK
[3]Centre for Novel Agricultural Products (CNAP), Department of Biology, University of York, Heslington, York YO10 5DD, UK
[4]Co-first authors

*Correspondence:
luke.mackinder@york.ac.uk (L.C.M. Mackinder) and
Alistair.McCormick@ed.ac.uk (A.J. McCormick).

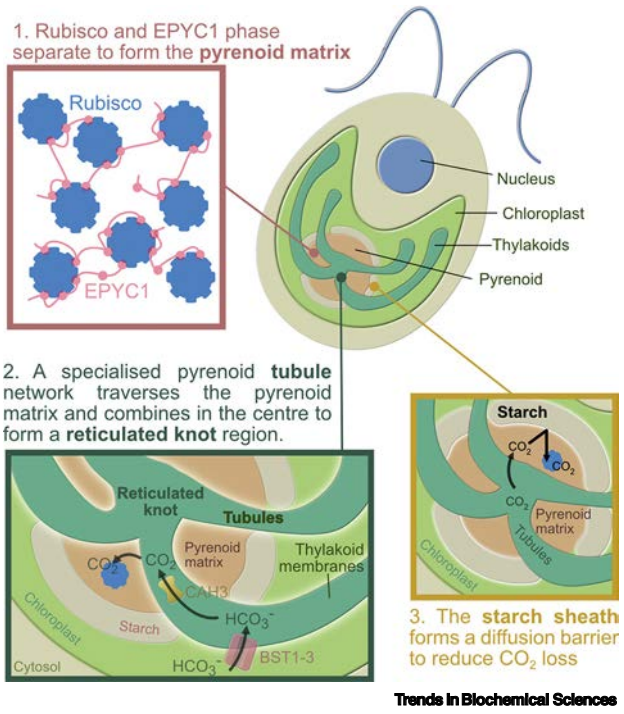

Figure 1. Three key architectural features of the pyrenoid-based CO_2-concentrating mechanism in *Chlamydomonas*. (1) The pyrenoid matrix predominantly comprises ribulose-1,5-bisphosphate carboxylase/oxygenase (Rubisco) and the Rubisco-linker protein EPYC1, which binds to the small subunit of Rubisco and facilitates the formation of a phase-separated liquid-like condensate. (2) The pyrenoid matrix is traversed by a network of pyrenoid tubules, which converge in the centre of the matrix to form a reticulated knot-like region (see Figure 2 in the main text for more details). The tubules are contiguous with the wider chloroplast thylakoid membrane network and facilitate delivery of CO_2. Bicarbonate (HCO_3^-) in the chloroplast stroma diffuses through bestrophin-like channels (BST1–3) into the thylakoid lumen. In the lumen, carbonic anhydrase 3 (CAH3) converts HCO_3^- into CO_2, which subsequently diffuses into the pyrenoid matrix to be fixed by Rubisco. (3) CO_2 in the pyrenoid matrix is prevented from diffusing away by a starch sheath, which forms a diffusion barrier around the pyrenoid.

gather in the centre of the pyrenoid to form a reticulated knot-like structure. Bicarbonate (HCO_3^-) is channelled into the pyrenoid tubules from the stroma, likely via **bestrophin-like proteins (BSTs)** enriched in thylakoid regions at the periphery of the matrix [21], and then converted back into CO_2 by the lumenal carbonic anhydrase CAH3 located in the pyrenoid tubules [22,23]. This generates a localised source of CO_2 that diffuses into the surrounding **pyrenoid matrix** for capture by Rubisco. Third, a sheath of starch plates surrounds the matrix, potentially to limit diffusion of CO_2 away from the matrix [24,25]. Overall, molecular-scale modelling indicates that these structures can facilitate a threefold increase in CO_2 fixation rate [26].

Here, we review recent advances in our molecular knowledge of the biogenesis of these three architectural features, how they enhance the concentration of CO_2 in the Rubisco matrix, and how the pCCM is energized. We then highlight ongoing efforts to assemble functional pyrenoids into plants, which has helped to reveal much about the operation of the pCCM and its component proteins in *Chlamydomonas*.

Biomolecular condensation of Rubisco to form the pyrenoid matrix

Liquid–liquid phase separation (LLPS) underpins the assembly of the pyrenoid matrix in *Chlamydomonas* (Box 1), which forms through complex coacervation between Rubisco and the **intrinsically disordered** linker protein EPYC1 [27,28]. EPYC1 contains five near-identical ~60 amino acid repeats. Each repeat contains a short helical **Rubisco-binding motif (RBM)** (sticker) and a longer disorder-promoting sequence (**spacer**), which provides flexibility between the **stickers** (Figure 2). The stickers on EPYC1 bind to the small subunit of the hexadecameric Rubisco complex (comprising eight large and eight small subunits; L8S8); thus, theoretically, EPYC1 can bind to up to five different Rubisco molecules and each Rubisco can bind up to eight different EPYC1 molecules [29]. In line with LLPS theory, the stickers have a weak affinity

Glossary

Bestrophin-like protein (BST): protein with structural similarity to bestrophins. Bestrophins are found in a wide diversity of organisms, where they act as anion channels, with permeability to chloride and bicarbonate (HCO_3^-), among other anions.
C3 plants: plants that utilise C3 photosynthesis, in which the first major carbon compound produced contains three carbon atoms.
CO_2-concentrating mechanism (CCM): set of molecular components that increase the concentration of CO_2 around Rubisco to improve its efficiency.
Intrinsically disordered (protein): proteins that lack a well-defined 3D structure.
Liquid–liquid phase separation (LLPS): separation of a mixture of components into two liquid phases.
Protopyrenoid: pyrenoid-like matrix comprising EPYC1 and hybrid Rubisco consisting of the *Chlamydomonas* small subunit and plant (*Arabidopsis*) large subunit.
Proxiome: collection of proteins found in close proximity to a particular target protein.
Pyrenoid matrix: in *Chlamydomonas*, a liquid–liquid phase-separated condensate formed by the interaction of EPYC1 and Rubisco. The matrix contains several other proteins, such as Rubisco activase.
Pyrenoid tubules: specialised thylakoid membranes that traverse the pyrenoid matrix.
Rubisco-binding motif (RBM): common amino acid sequence found in proteins localising to the pyrenoid in *Chlamydomonas*. The motif interacts with two alpha-helices on the small subunit of Rubisco.
Spacers: regions of a protein (typically disordered) involved in LLPS that do not engage in the protein–protein interactions required for phase separation.
Starch sheath: arrangement of starch plates that forms around the periphery of the pyrenoid matrix in *Chlamydomonas* and many other pyrenoid-containing organisms. Models suggest it acts as a barrier to reduce diffusional loss of CO_2.
Stickers: protein regions involved in the protein–protein interactions that drive phase separation.

(K_d = 3 mM) but multivalent binding enables LLPS and the observed properties of the *Chlamydomonas* pyrenoid [26,28,29].

In vitro and *in planta* work has shown that the presence of EPYC1 and the *Chlamydomonas* Rubisco small subunit (or a '*Chlamydomonas*-like' small subunit) is sufficient to induce phase separation, with condensates in plants being dubbed '**protopyrenoids**' (Figure 3A) [14,18]. Although Rubisco (Form I) is a somewhat unusual component for LLPS given its rigid cuboid shape [28], the quaternary structure of the L8S8 complex provides a large surface area, which has likely allowed for both specific and nonspecific interactions to evolve that can facilitate condensate formation (for further review, see [30]). A wealth of evidence supports the LLPS behaviour of the *Chlamydomonas* pyrenoid. The arrangement of Rubisco within the matrix has been modelled as being similar to the distribution of molecules within a fluid [19,30]. Pyrenoid division is coordinated with chloroplast cell division and, before pyrenoid division via fission, rapid partial dissolution of the pyrenoid takes place, partitioning more Rubisco into the dilute phase (i.e., outside of the pyrenoid in the chloroplast stroma). Once divided, the stromal Rubisco rapidly recondenses within 1 min back into the pyrenoid in daughter cells. This can take place via nucleation, and then fusion, of smaller Rubisco assemblies, or by a process called Ostwald ripening, where Rubisco moves from smaller condensates to larger ones [30]. In addition, fluorescence recovery after photobleaching (FRAP) experiments have shown that the three major matrix components [Rubisco, Rubisco activase (Rca), and EPYC1] are mobile on the timescale of seconds within the condensate [19]. Many of these LLPS properties have also been recapitulated *in vitro* and *in planta* [14,18].

How pyrenoid dissolution and condensation is controlled in *Chlamydomonas* remains unknown. However, it has been proposed that both EPYC1 and Rubisco in the dilute and dense phases are regulated by post-translational modifications that could influence binding affinities and,

Box 1. The basics of biological liquid–liquid phase separation

Biological LLPS is a key process for pyrenoid biogenesis and function. It can compartmentalise cellular processes and concentrate specific (bio)molecules. These compartments include P granules, nucleoli, Cajal bodies, and stress granules [72], with many additional structures and processes in both eukaryotes and prokaryotes proposed to be underpinned by LLPS [73,74].

The biological LLPS field uses concepts from polymer chemistry and soft matter physics. Proteins/nucleic acids are considered to be polymers in solution that can separate into a dense phase (condensate) and a dilute phase [72]. Two modes of action are associated with the creation of biomolecular condensates: (i) interactions via no-specific weak interactions (charge–charge, π–π, cation–π, hydrophobic contacts, and hydrogen bonds [75]; or (ii) multivalent binding of structured domains separated by disordered linker domains [39]. To unify these modes across scales, a 'sticker' and 'spacer' model was proposed (Figure IA) [76,77]. Stickers provide interactions, while spacers separate them and tune the solubility of the protein and condensate properties [76,77]. Proteins that are sufficient and necessary to form condensates are termed 'scaffolds' or 'drivers', such as G3BP in stress granules [78] or NPM1 in nucleoli [79], whereas proteins partitioning into condensates are called 'clients' [80]. Homotypic separation is driven by a single biomolecule species, while heterotypic separation occurs where two or more different biomolecules are required for LLPS (i.e., the complex coacervation seen in pyrenoids). Phase diagrams illustrate conditions needed for phase separation, which are typically shown as a function of protein concentration against a specific condition (e.g., pH, temperature, or salt) (Figure IB).

LLPS offers several advantages compared with membrane-bound or cross-linked organelles. The phase boundary can provide an energy barrier to partition certain biomolecules and exclude others without using membranes. This can increase the specificity for biochemical reactions, such as Rubisco carboxylation in the pyrenoid. The liquid properties of biomolecular condensates allow for enhanced diffusion of substrates to enzymes, the ability to buffer biomolecule concentrations, and rapid responses to changing environmental parameters [80].

Whether condensates are formed via LLPS or alternative active processes requires thorough *in vitro* and *in vivo* evidence, with many proposed LLPS systems recently questioned [81,82] and the importance of LLPS unclear for others. By contrast, the *Chlamydomonas* pyrenoid provides a clear picture of phase separation driven by the interactions of two multivalent proteins: Rubisco and EPYC1. Both are necessary and sufficient for LLPS [18,27,36], and biologically relevant for cell survival at atmospheric CO_2 levels. Thus, the pyrenoid is an elegant model for investigating LLPS both *in vitro* and *in vivo*.

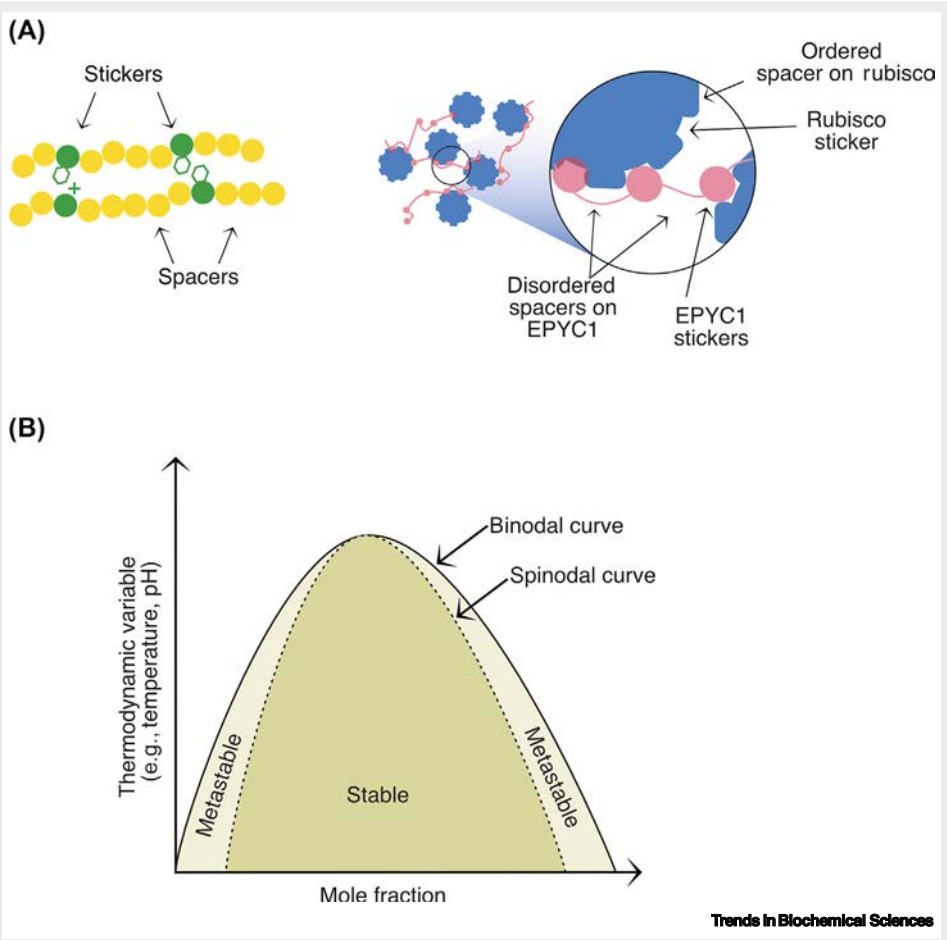

Figure I. The stickers and spacers model applied to the *Chlamydomonas* pyrenoid. (A) The stickers and spacers framework can describe the underlying structural principles of phase separation at different scales. Nonspecific interactions, such as π–cation and π–π interactions between amino acids in a disordered protein region, serve as stickers (green residues), while the noninteracting amino acids are spacers (yellow residues). In the case of folded proteins, interacting domains are considered stickers, while the spacers are disordered regions between them [e.g., the disordered sequences separating the short helical ribulose-1,5-bisphosphate carboxylase/oxygenase (Rubisco)-binding motifs (RBMs) in EPYC1 in pink] or can be structured regions (e.g., in the case of Rubisco in blue). (B) Phase diagrams are used to describe the thermodynamic conditions under which phase separation occurs. The binodal curve separates the metastable state, where two phases can coexist and demixing will occur via nucleation and growth, from stable states (outside of the curve), where the components form one phase. The space under the spinodal curve describes the conditions where one phase is unstable and phase separation occurs spontaneously via spinodal decomposition.

hence, phase diagrams [31]. For example, EPYC1 phosphorylation may reduce sticker binding affinity, thus increasing the required saturation concentration for condensation, resulting in pyrenoid dissolution. Such a process would enable the rapid (i.e., faster than transcription or translation) matrix assembly and disassembly observed in *Chlamydomonas* [30]. Until recently, it was unclear whether EPYC1 and Rubisco also interacted in the dilute phase. Two independent studies have now shown that, at least *in vitro*, EPYC1 and Rubisco do interact to form small oligomers in the dilute phase separate from the denser condensate [31,32]. Below the concentration threshold for condensation, EPYC1–Rubisco complexes typically contain only a single Rubisco, although at higher EPYC1 concentrations, multiple EPYC1 molecules can bind a single Rubisco. Evidence for EPYC1–Rubisco complex formation in the dilute phase remains lacking *in vivo* but should be

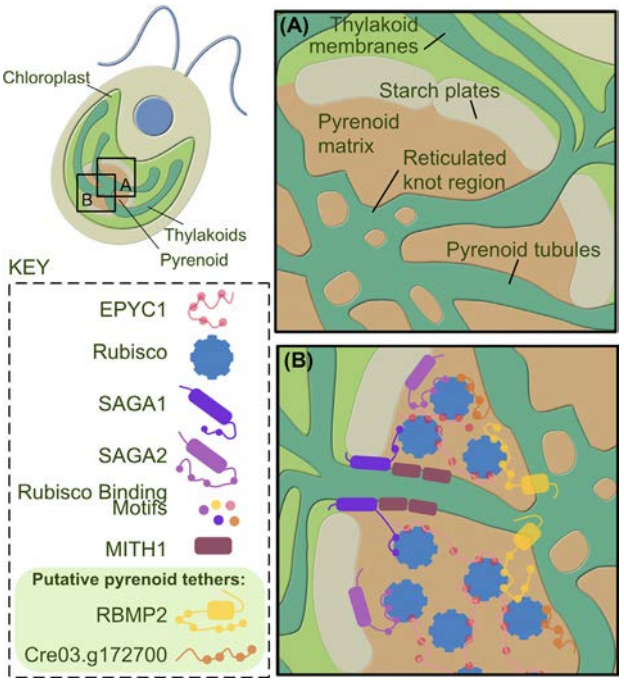

Figure 2. Components involved in pyrenoid assembly in *Chlamydomonas*. (A) The structure of the pyrenoid is characterised by a dense, phase-separated matrix, surrounded by a sheath of starch plates. Thylakoid membranes fuse at the pyrenoid periphery and enter through gaps between the starch plates, where they tubularise and traverse the pyrenoid matrix to meet in a central reticulated knot. (B) The structure of the pyrenoid is maintained by proteins that share a common ribulose-1,5-bisphosphate carboxylase/oxygenase (Rubisco)-binding motif (RBM) [36]. The matrix is held together by multivalent interactions between the linker protein EPYC1 and Rubisco, which facilitate phase separation. STARCH GRANULES ABNORMAL (SAGA)-1 and SAGA2 are large predominantly disordered proteins containing both carbohydrate-binding domains and RBMs that recruit starch to the pyrenoid. SAGA2 localises to the interface between the matrix and the starch sheath, whereas SAGA1 localises *in puncta* at the points of thylakoid entry to the pyrenoid. SAGA1 also makes contact with the thylakoid membranes, recruiting MITH1, which then extends the thylakoids through the matrix. Further factors are required to tubularise the traversing membranes and form the reticulated knot at the centre. Pyrenoid tubule-localised proteins RBMP2 and Cre03.g172700 may contribute to the tethering of the Rubisco matrix to the tubules [34,36].

achievable using similar single molecule methods as applied *in vitro*. The implications for dilute phase binding are unclear, but are potentially important for understanding *de novo* pyrenoid assembly, which is seen in daughter cells that fail to inherit a pyrenoid due to incorrect pyrenoid fission [32].

The interactions between EPYC1 and the *Chlamydomonas* Rubisco small subunit are now well characterised, but less is known about the association of the other 30–84 predicted proteins within the *Chlamydomonas* pyrenoid [13,33–35]. RBMs are a common feature of many pyrenoid-localised proteins [36]. Approximately 43% of a TurboID generated high-confidence pyrenoid **proxiome** (30 proteins) contain RBMs [34], supporting a central assembly role for Rubisco. Several more recently discovered RBM-containing components may have key roles in Rubisco maintenance, including Cre16.g655050, a highly disordered protein with a predicted N-terminal RbcX fold that may have a Rubisco chaperone role [13].

What of the proteins that do not have any predicted RBMs? For example, Rca is highly enriched in the pyrenoid but lacks an RBM and still binds Rubisco through transient interactions with the large subunit, a distinct interface from the EPYC1-binding region [37]. CPLD2 (Cre03.g206550) is a homolog of plant xylulose-1,5-biphosphate (XuBP) phosphatase that consumes XuBP, a misfire product of Rubisco and potent inhibitor of the enzyme [35,38]. Enrichment of CPLD2 in the matrix could allow for rapid removal of XuBP from the Rubisco pool and, thus, increase the total potential Rubisco activity for CO_2 fixation. Additional examples could exist that do not rely on direct Rubisco interactions. SAGA2 interacts not only with CrRbcS through four RBMs, but also with EPYC1 [13,15], suggesting that other non-RBM domains help recruit proteins to the pyrenoid. Several characteristics determine whether a protein can undergo phase separation,

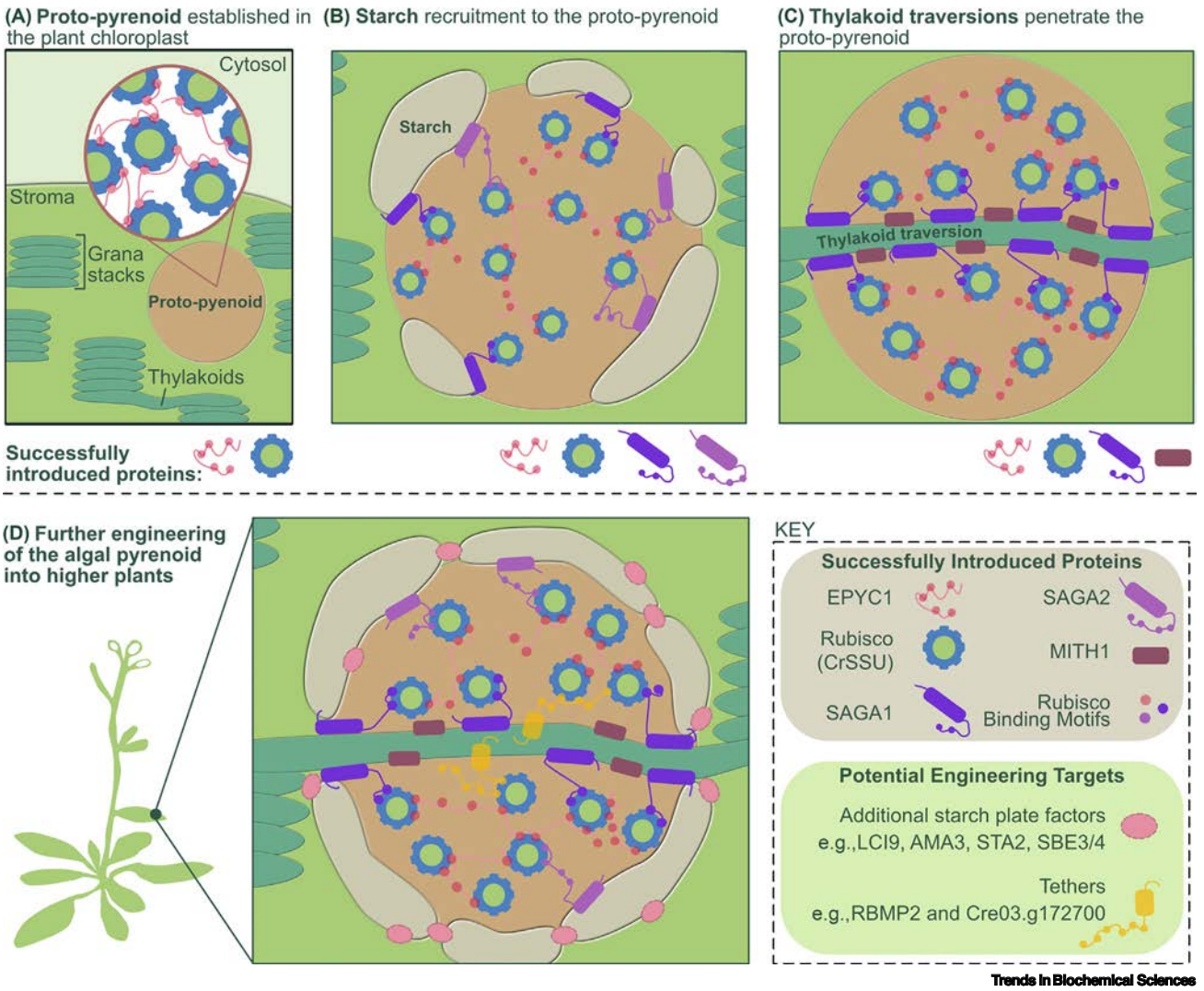

Figure 3. Progress toward engineering pyrenoid architecture in plant chloroplasts. Establishing a functional pyrenoid-based CO2-concentrating mechanism (pCCM) in a C3 plant is predicted to increase CO_2 fixation capacity in the chloroplast by up to threefold [26]. The following assembly steps demonstrate recent achievements in assembling the architecture of a pyrenoid in the model plant *Arabidopsis thaliana*. (A) A liquid–liquid phase-separated 'protopyrenoid' matrix is generated by expressing the *Chlamydomonas* linker protein EPYC1 in *Arabidopsis* containing pyrenoid-compatible hybrid ribulose-1,5-bisphosphate carboxylase/oxygenase (Rubisco) comprising *A. thaliana* large subunits and *Chlamydomonas* small subunits [14]. (B) Starch is recruited to the protopyrenoid by expressing the *Chlamydomonas* proteins STARCH GRANULES ABNORMAL (SAGA)-1 and SAGA2. Irregularly shaped starch granules surround and curve around the matrix periphery [15]. (C) Concurrent expression of tubule biogenesis proteins SAGA1 and MISSING THYLAKOIDS 1 (MITH1) drives the formation of one or more sheet-like thylakoid traversions across the protopyrenoid matrix. SAGA1 and MITH1 localise along the traversing membrane [43]. (D) Future efforts will focus on combining a starch sheath and thylakoid traversions through the protopyrenoid. Modelling shows that an efficient pCCM requires a starch diffusion barrier to prevent leakage of CO_2 from the pyrenoid matrix [26]. Additional starch metabolism and/or binding components will likely be required to shape the starch granules. Thylakoid traversions will allow the delivery of CO_2 to the protopyrenoid matrix and may require the expression of additional pyrenoid tethers.

including the presence of disordered or low-complexity domains, charge patterning, and amino acid composition [19,39,40].

Whether all pyrenoids are formed via LLPS remains an open question. Microscopy observations from a range of algae and hornwort species suggest that many pyrenoids display liquid-like behaviour [3,6]. Additionally, *in vitro* reconstitution of the Rubisco matrix from the diatom *Phaeodactylum*

tricornutum and the green alga *Chlorella sorokiniana* supports LLPS of divergent pyrenoids. However, the rigidity of the matrix varies between species both *in vitro* and *in vivo* [7,9,10].

Insights into the formation of the pyrenoid-traversing thylakoid network

Currently, little is known about the biogenesis of *Chlamydomonas* pyrenoid tubules. Due to the relative complexity of the network (including the presence of apparent 'minitubules' within each tubule [20]), multiple components may be involved, including membrane remodelling proteins for tubule formation, proteins involved in establishing the network architecture, and tether proteins to link the tubules to the Rubisco matrix [20,29]. For the latter, several RBM-containing proteins that localise to the tubule network have been identified, including BST4 (previously RBMP1), RBMP2, and, more recently, Cre03.g172700, with both BST4 and RBMP2 containing predicted transmembrane domains [13,34,36].

BST4 contains a conserved bestrophin domain similar to the putative bestrophin-like HCO_3^- channels BST1-3 [21] (Figure 1), but also has an extended disordered C terminus containing two RBMs [36], which suggests a potential dual function for BST4 as a tether and an anion channel. However, recent work in *Chlamydomonas* has shown that pyrenoid structure and the thylakoid network appear unaffected by the absence of BST4. Furthermore, heterologous expression of BST4 in transgenic *Arabidopsis* engineered to produce protopyrenoids showed that BST4 was enriched in the thylakoid stromal lamellae surrounding the protopyrenoid, but was not present in the Rubisco matrix. Subsequent transmission electron microscopy (TEM) imaging confirmed that there were no thylakoids traversing the matrix, indicating that BST4 was not sufficient to drive thylakoid incorporation *in planta*. Overall, these data suggest that BST4 is either not a tether protein or has a redundant tethering role in *Chlamydomonas*. Additional characterisation work revealed that BST4 may have a role in regulating oxidative stress within the pyrenoid tubules. Thus, BST4 may help to coordinate the light reactions with CO_2 fixation under pCCM-induced conditions [41].

RBMP2 contains six RBMs, the most identified in a pyrenoid-localised protein to date [13]. Compared with BST4, RBMP2 localises more centrally in the pyrenoid tubule network within the reticulated knot region [17,36]. Cre03.g172700 is predicted to be a largely disordered protein that contains four RBMs [34]. Based on its subpyrenoid localisation, Cre03.g172700 may be associated with the pyrenoid tubules. RBMP2 and Cre03.g172700 have yet to be validated as bona fide tethers that link the tubules and Rubisco matrix, although they appear to be strong candidates. *In planta* engineering work with RBMP2 has thus far been limited due to low transgene expression [15].

More recently, STARCH GRANULES ABNORMAL (SAGA1) and MISSING THYLAKOIDS 1 (MITH1, previously SAGA3 [42]) were identified as central regulators in the initiation of thylakoid traversions through the matrix (Figure 2B) [43]. SAGA1 localises in puncta at the interface between the matrix and the **starch sheath**, potentially at the entry points of the pyrenoid tubules between the starch plates. Previous work showed that SAGA1 is a crucial component for normal starch sheath morphology and pyrenoid formation, because *saga1* mutants have multiple pyrenoids, most of which lack a thylakoid tubule network [24]. MITH1 is a homolog of SAGA1, which localises to the tubules, and *mith1* mutants display a CCM-defective phenotype similar to that of *saga1*. Crucially, *mith1* has no tubules traversing across the pyrenoid, although thylakoid membranes were observed to cross the starch sheath and stop at the edge of the matrix. Hennacy *et al.* proposed a model whereby SAGA1 facilitates tubule biogenesis on the surface of the matrix [43] and MITH1 then draws the membranes through the pyrenoid. This hypothesis was directly supported by co-expression of MITH1 and SAGA1 in transgenic *Arabidopsis* protopyrenoid lines, which led to the formation of thylakoid membrane traversions through the protopyrenoid matrix (Figure 3C). Thus, SAGA1 and MITH1 appear necessary and sufficient to induce thylakoid traversions.

Notably, the traversions *in planta* retained a sheet-like appearance similar to typical plant thylakoid membranes [43]. Thus, it is likely that the components involved in tubule formation and maturation in *Chlamydomonas* remain to be discovered. Two candidates have already emerged [34]. STRUCTURAL MAINTENANCE OF CHROMOSOMES 7 (SMC7) has a comparable localisation to SAGA1 and could work through a similar mechanism. Cre09.g394510 also lines the matrix–starch interface and contains a t-snare domain, known for acting in vesicle fusion [34,44]. Thus, Cre09.g394510 may have a role in the remodelling of thylakoid membranes into pyrenoid tubules.

Although tubules are present in the *Chlamydomonas* pyrenoid, many other pyrenoid-containing species (such as *C. sorokiniana* and the model diatom *P.* tricornutum [7,9]) retain 'simpler' sheet-like thylakoid traversions that lack minitubules, akin to those observed in transgenic *Arabidopsis* [3,43]. From a plant engineering perspective, this is encouraging because reconstitution of the complex pyrenoid tubule network observed in *Chlamydomonas* may not be essential for assembling a functional pCCM in plants.

How does *Chlamydomonas* build a starch sheath?

An efficient pCCM requires a robust CO_2 diffusion barrier around the Rubisco matrix to minimise CO_2 leakage [26]. In *Chlamydomonas* and several other algae, the CO_2 diffusion barrier is formed by a sheath of starch plates. Although the requirement for a starch sheath for a functional pCCM in *Chlamydomonas* has been debated [45], recent experimental evidence and modelling support that the starch sheath is necessary to maintain elevated CO_2 concentrations in the matrix [25,26]. The morphology of the sheath varies dramatically between species, from a single plate to two, or more commonly, multiple plates [3]. Species that lack a starch sheath (e.g., some hornworts and diatoms) may limit CO_2 leakage by surrounding the pyrenoid with tightly packed thylakoid membranes [6] or, as recently discovered in diatoms, a proteinaceous sheath of pyrenoid shell (PyShell) proteins [8,10]. Although the effectiveness of the latter strategies is still to be determined, modelling of the cyanobacterial CCM shows that the carboxysome protein shell provides a highly efficient barrier for CO_2 retention [46], while Fei *et al.* predicted that a starch sheath could retain up to 33% more CO_2 in the Rubisco matrix compared with appressed thylakoid membranes [26]. Thus, for engineering a functional pCCM into plants, it appears that there are several ways to build a CO_2 diffusion barrier around the Rubisco matrix.

Understanding how the curved starch plates in *Chlamydomonas* form is an ongoing area of research, but SAGA1 and SAGA2 appear essential for normal starch plate biogenesis (Figures 2 and 3) [24,36]. Both proteins contain RBMs and an N-terminal starch-binding domain (CBM20), and both are proposed to co-mediate interactions between the matrix and the starch sheath. SAGA1 at least appears to have a multifaceted role in the *Chlamydomonas* pCCM. As highlighted in the previous section, SAGA1 is also important for the initiation of the traversing thylakoid tubule network [43], but is additionally necessary for the expression of numerous pCCM genes and appropriate localisation of the important stromal carbonic anhydrase LCIB [47,48]. However, these could be pleiotropic effects driven by a breakdown of pyrenoid function due to incorrect pyrenoid tubule assembly.

Atkinson *et al.* recently expressed SAGA1 in transgenic *Arabidopsis* protopyrenoid lines and observed that SAGA1 not only localised to the matrix, but was also sufficient to recruit starch [15]. Furthermore, expression of SAGA1 produced a nonlipid based 'network structure' within the matrix. Expression of both SAGA1 and SAGA2 resulted in >70% of chloroplast starch associating with the protopyrenoid, with large, plate-like starch granules observed around the edges of the matrix (Figure 3B). In some cases, these granules completely encircled the protopyrenoid in a conformation resembling the starch sheath in *Chlamydomonas*.

Further plant engineering work will be required to build a starch barrier that more fully encases the matrix and allows insertion points for the traversing thylakoids. There are several candidates already available that could help to achieve this. LCI9 is a protein with two CBM20 domains, which localises between the starch plates and the pyrenoid matrix and may have role in coordinating plate growth and positioning [13]. ALPHA AMYLASE 3 (AMA3) is a starch-metabolising enzyme located in the pyrenoid and is enriched in response to low CO_2 [34]. The expression of these proteins and/or other starch-associated proteins, such as STA2, SBE3, or SBE4, which localise to the pyrenoid and are thought to help shape the starch granules, could help to further develop a protopyrenoidal starch sheath.

Delivery of inorganic carbon to the pyrenoid

Rubisco in the pyrenoid matrix requires a regular supply of CO_2 to meet its carbon fixation potential. This involves the uptake of inorganic carbon (Ci; CO_2, HCO_3^-, H_2CO_3, and CO_3^{2-}) from the external environment and its transport into the pyrenoid tubules to be delivered as CO_2 to the matrix (Figure 4). The uptake system is under the control of a transcriptional regulator, CIA5, which upregulates many of the CCM genes under CO_2-replete conditions [49–51]. In addition, the CO_2 delivery pathway to the *Chlamydomonas* pyrenoid changes depending on CO_2 availability.

Under very-low CO_2 ($VLCO_2$) conditions (<0.03% CO_2), the CCM largely relies on the uptake of HCO_3^- from the extracellular environment (Figure 4A). Given that membranes do not easily facilitate the diffusion of anions, HCO_3^- uptake relies on a series of channel proteins. High light-activated protein-3 (HLA3), an ATP-binding cassette (ABC) transporter, is thought to facilitate HCO_3^- transport across the plasma membrane [16,52–55]. HLA3 forms a complex with autoinhibited Ca^{2+} protein 4 (ACA4) [12], a plasma membrane H^+-ATPase in group IIIA, which is known to be involved in H^+ export while expending ATP [56]. Given that ACA4 is likely generating alkaline conditions in the cytosol immediately adjacent to the plasma membrane, this may prevent the dehydration of HCO_3^- to CO_2 and its subsequent leakage out of the cell. Alternatively, or in combination, the acidification of the periplasmic space may increase the CO_2 in the extracellular environment.

HLA3 expression is co-regulated with the chloroplast envelope channel low carbon-inducible gene (LCI)-A [47,56]. LCIA is a formate/nitrate transporter, which is thought to facilitate HCO_3^- passage out of the cytosol into the chloroplast stroma. The activity of LCIA as a HCO_3^- channel has been documented in a range of heterologous systems [16,47,57], most recently *in planta* [58]. Stromal HCO_3^- is then channelled into the lumen of the thylakoid membranes, likely by three homologous BSTs (BST1–3) [21]. BSTs are passive anion channels [59] that rely on the concentration gradient between the slightly alkaline stroma (~pH 8) and the acidified lumen (~pH 5.5). Once in the thylakoid lumen, HCO_3^- is dehydrated to form CO_2 by CAH3 located within the pyrenoid tubules, whereafter CO_2 diffuses out into the surrounding matrix. BST1–3 and CAH3 are enriched in the pyrenoid tubules at the pyrenoid periphery and within the pyrenoid, respectively [22,23,60]. Modelling predicts that the localisations of BST1–3 and CAH3 are key for the efficient delivery of CO_2 to Rubisco in the pyrenoid matrix [26].

Although the pyrenoid starch sheath helps to reduce CO_2 leakage, some CO_2 is thought to escape the pyrenoid matrix into the chloroplast stroma, which then must be recaptured by a stromal CA by catalysing its hydration back into HCO_3^-. Previous work has provided indirect evidence that LCIB was key to this recovery [59], but only recently has the CA activity of LCIB been demonstrated, albeit indirectly, in yeast and plant heterologous systems [61]. LCIB forms an hexameric complex with the homologous protein LCIC in the stroma. Although LCIC has not been shown to have CA activity, it has been indirectly implicated in the relocalisation of LCIB under $VLCO_2$ conditions [46].

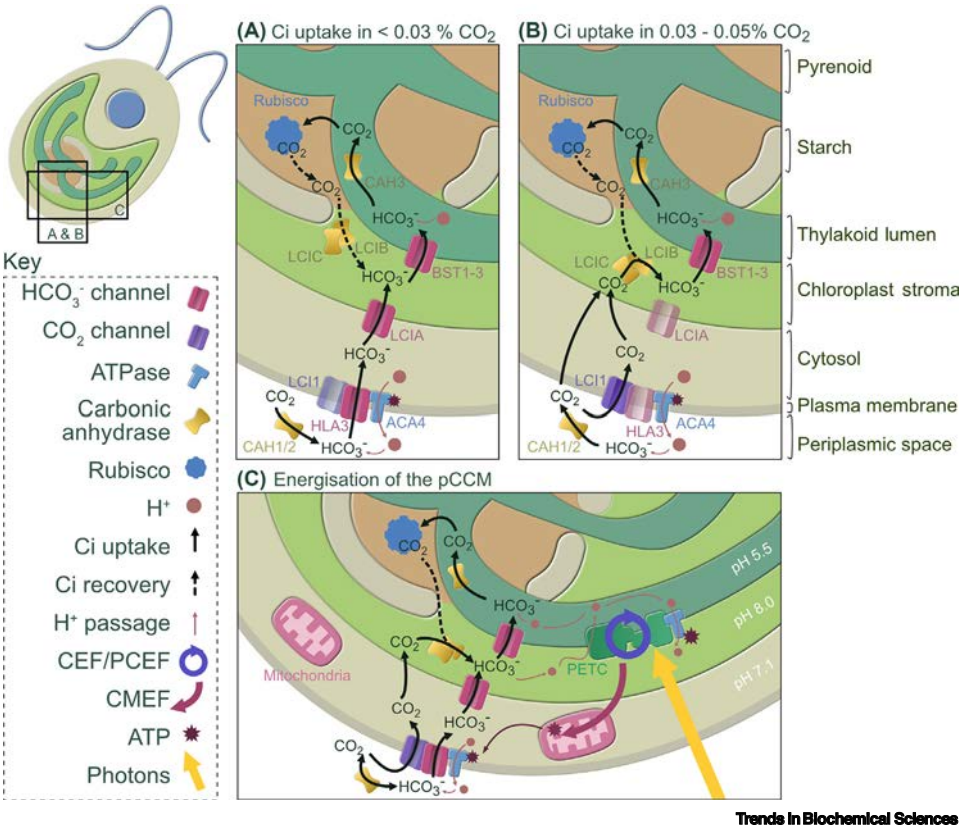

Figure 4. Pathways of inorganic carbon (Ci) delivery to the pyrenoid matrix. (A) Under very low (<0.03%) CO_2 ($VLCO_2$) conditions, external Ci is predominantly taken up in the form of bicarbonate (HCO_3^-) through high light-activated protein-3 (HLA3). HCO_3^- is then channelled across the chloroplast envelope via LCIA and down a pH-driven HCO_3^- gradient into the thylakoid lumen via BST1–3. In the lumen, HCO_3^- is dehydrated by CAH3 enriched in the pyrenoid tubules, generating CO_2, which diffuses out into the matrix for fixation by ribulose-1,5-bisphosphate carboxylase/oxygenase (Rubisco). CO_2 that diffuses away from the matrix is recaptured as HCO_3^- by low carbon-inducible gene (LCI)-B, which relocalises to the pyrenoid periphery under $VLCO_2$ conditions. (B) In ambient CO_2 (0.03–0.05% CO_2), Ci uptake is predominantly in the form of CO_2, which passes through LCI1 or diffuses through the plasma membrane. CO_2 travels down its concentration gradient, crossing the chloroplast envelope either by diffusion or an as-yet unidentified CO_2 channel. CO_2 is then converted to HCO_3^- by LCIB, which is more diffuse throughout the chloroplast at ambient CO_2, to maintain the concentration gradient. HCO_3^- then enters the thylakoid lumen as in (A). (C) Ci uptake is energised by a combination of photons, electrons, and ATP. Photosynthetic cyclic and pseudo-cyclic electron flow (CEF and PSEF) use photons and electron transport to generate protons. These protons acidify the lumen and drive the uptake of HCO_3^- through bestrophin-like proteins (BST1–3) and facilitate its dehydration to CO_2 by carbonic anhydrase 3 (CAH3). CEF and PSEF also provide protons for ATP production by thylakoid membrane ATPase. Mitochondria are another source of ATP and are thought to use photosynthetic reducing power for ATP generation, a process known as chloroplast-mitochondrial electron flow (CMEF) [64]. ATP is needed for active Ci uptake by directly driving HCO_3^- uptake by HLA3 at the plasma membrane and/or indirectly by modifying CO_2:HCO_3^- ratios by driving the export of protons through autoinhibited Ca^{2+} protein 4 (ACA4).

Under ambient CO_2 conditions (0.03–0.5% CO_2), there are key differences to the Ci delivery pathway (Figure 4B). First, Ci predominantly enters the cell through the passive diffusion of CO_2 across the plasma membrane. Some CO_2 has also been shown to be actively transported into the cell by LCI1, a CO_2 channel localised to the plasma membrane [60,62], which interacts with HLA3 [13]. Cytosolic CO_2 is then thought to diffuse across the chloroplast envelope into the stroma, where it is converted to HCO_3^- by LCIB. This maintains the CO_2 gradient from the cytoplasm, enables the concentration of Ci in the stroma, and prevents CO_2 from leaking from the cell. HCO_3^- can then

enter the thylakoid lumen through BST1–3 and continue as described above. This pathway is said to be LCIB dependent, because the absence of LCIB under ambient CO_2 is lethal for cell survival [63].

How is the pCCM Ci delivery pathway energised?

Understanding the energetic processes that enable the delivery of Ci to the pyrenoid is a key focus of recent research. pCCM energisation relies on a combination of photons (light), electrons, and ATP generated by pseudo-cyclic electron flow (PCEF), cyclic electron flow (CEF), and chloroplast-mitochondrial electron flow (CMEF) [64]. In brief, PCEF and CEF are energised by light and generate protons that accumulate in the lumen [65–67], which help to drive the pCCM (Figure 4C). Proton accumulation acidifies the lumen, generating an electrochemical gradient that allows for uptake of HCO_3^- by BST1–3. The protons are also available to CAH3 to catalyse the dehydration of HCO_3^- into CO_2 [21,68]. PCEF and CEF are thought to be sufficient not only to drive Ci flow in the pCCM, but also to provide a sufficient proton pool for ATP production by ATPase [65,68].

Mitochondria are also closely connected to the energisation of the pCCM and relocalise to the periphery of the chloroplast under ambient CO_2 conditions [69]. A recent study observed a decrease in Ci affinity when mitochondrial activity was inhibited [68], which was attributed to decreased CMEF (i.e., the reducing power produced by photosynthetic electron transport is transferred from the chloroplast stroma to the mitochondria to generate ATP). The latter ATP is important to facilitate the active transport mechanisms of Ci uptake, such as ATP utilised by ACA4 and HLA3 at the plasma membrane.

The energy transfer between these metabolic processes is likely complex. Photosynthesis not only energises the pCCM, but also places demands on the Ci budget of the cell. For example, exposure to high light causes an increase in NADPH and ATP, which enables more flux through the Calvin cycle, and increases Ci demand. This results in upregulation of the pCCM components to compensate for the increased Ci demand and to cope with excess light energy in a manner that does not harm the cell. The pCCM master regulator CIA5 not only controls key pCCM components, but is also able to regulate the photoprotective response of *Chlamydomonas* to high light [69–71]. These studies show that, while we do not yet fully understand the mechanisms behind the integration of the CCM into wider cellular processes, the field is now starting to address these knowledge gaps, and we anticipate significant advances in the near future.

Concluding remarks

Although significant recent successes have been made in developing the architecture of the pyrenoid *in planta*, next key challenges for functionalising the pCCM include examining and appropriately localising the activities of BST1–3 and CAH3 in plants, and investigating whether the energisation requirements of the pCCM are compatible with plant mesophyll chloroplasts (and mitochondria) (also see Outstanding questions). Current modelling efforts predict that an engineering approach using a minimal set of components is feasible to develop a basic functional plant-based pCCM, which could lead to enhanced crop productivities and resilience to environmental stresses [24]. Future testing of this model and the development of future models will help inform the Design–Build–Test–Learn cycle in this exciting field of engineering biology research.

Outstanding questions

What components are required for tubularisation of the pyrenoid tubules in *Chlamydomonas* and the generation of the central reticulated knot?

How crucial are pyrenoid tubules for pCCM function?

Are minitubules found in algae other than *Chlamydomonas*, and if so, to what extent?

Are pyrenoid tubules necessary for engineering a pCCM into plants or would sheet-like pyrenoid-traversing thylakoids similar to those observed in other species be sufficient?

How is the pyrenoidal starch sheath shaped in *Chlamydomonas*, and which proteins will be required to establish a more complete starch barrier around a pCCM *in planta*?

How do proteins without Rubisco-binding motifs localise to the pyrenoid?

What role does post-translational modification have in directing pyrenoid assembly?

What is the mechanistic role of BST4 in the pyrenoid?

Are the energisation requirements of a plant-based pCCM compatible with plant mesophyll chloroplasts?

How does CAH3 localise to the pyrenoid, and can CAH3 activity be appropriately localised *in planta*?

Do regulatory mechanisms of pyrenoid division, growth, and dissolution, as seen in *Chlamydomonas*, need to be engineered in plants?

Acknowledgements

E.C. acknowledges funding from UK Research and Innovation EASTBIO DTP. S.M. was funded by a Biotechnology and Biological Sciences Research Council (BBSRC) studentship (BB/T007222/1). A.J.M. and L.C.M.M. acknowledge support from the UK Research and Innovation BBSRC (BB/Y000323/1), the Carbon Technology Research Foundation, Bill and Melinda Gates Foundation, and the Foreign, Commonwealth and Development Office. Additionally, A.J.M. acknowledges support from BBSRC grants BB/S015531/1, BB/X018377/1, and BB/W003538/1 and L.C.M.M. from a UKRI Future Leader Fellowship (MR/TO20679/1).

Declaration of interests

None declared by authors.

References

1. Flamholz, A.I. *et al.* (2019) Revisiting trade-offs between Rubisco kinetic parameters. *Biochemistry* 58, 3365–3376
2. Raven, J.A. *et al.* (2017) The possible evolution and future of CO_2-concentrating mechanisms. *J. Exp. Bot.* 68, 3701–3716
3. Barrett, J. *et al.* (2021) Pyrenoids: CO_2-fixing phase separated liquid organelles. *Biochim. Biophys. Acta Mol. Cell Res.* 1868, 118949
4. He, S. *et al.* (2023) The pyrenoid: the eukaryotic CO_2-concentrating organelle. *Plant Cell* 35, 3236–3259
5. Villarreal, J.C. and Renner, S.S. (2012) Hornwort pyrenoids, carbon-concentrating structures, evolved and were lost at least five times during the last 100 million years. *Proc. Natl. Acad. Sci. U. S. A.* 109, 18873–18878
6. Robison, T.A. *et al.* (2024) Hornworts reveal a spatial model for pyrenoid-based CO_2-concentrating mechanisms in land plants. *bioRxiv*, Published online June 30, 2024. https://doi.org/10.1101/2024.06.26/600872
7. Oh, Z.G. *et al.* (2023) A linker protein from a red-type pyrenoid phase separates with Rubisco via oligomerizing sticker motifs. *Proc. Natl. Acad. Sci. U. S. A.* 120, e2304833120
8. Shimakawa, G. *et al.* (2024) Diatom pyrenoids are encased in a protein shell that enables efficient CO_2 fixation. *Cell* 187, 1–16
9. Barrett, J. *et al.* (2024) A promiscuous mechanism to phase separate eukaryotic carbon fixation in the green lineage. *Nat. Plants*, Published online October 9, 2024. https://doi.org/10.1038/s41477-024-01812-x
10. Nam, O. *et al.* (2024) A protein blueprint of the diatom CO_2-fixing organelle. *Cell* 187, 5935–5950
11. Moromizato, R. *et al.* (2024) Pyrenoid protemics reveals independent evolution of the CO_2-concentrating organelle in chlorarachniophytes. *Proc. Natl. Acad. Sci. U. S. A.* 121, e2318542121
12. Li, X. *et al.* (2019) A genome-wide algal mutant library and functional screen identifies genes required for eukaryotic photosynthesis. *Nat. Genet.* 51, 627–635
13. Mackinder, L.C.M. *et al.* (2017) A spatial interactome reveals the protein organization of the algal CO_2-concentrating mechanism. *Cell* 171, 133–147
14. Atkinson, N. *et al.* (2020) Condensation of Rubisco into a proto-pyrenoid in higher plant chloroplasts. *Nat. Commun.* 11, 6303
15. Atkinson, N. *et al.* (2024) SAGA1 and SAGA2 promote starch formation around proto-pyrenoids in *Arabidopsis* chloroplasts. *Proc. Natl. Acad. Sci. U. S. A* 121, e2311013121
16. Atkinson, N. *et al.* (2016) Introducing an algal carbon-concentrating mechanism into higher plants: location and incorporation of key components. *Plant Biotechnol. J.* 14, 1302–1315
17. Adler, L. *et al.* (2022) New horizons for building pyrenoid-based CO_2-concentrating mechanisms in plants to improve yields. *Plant Physiol.* 190, 1609–1627
18. Wunder, T. *et al.* (2018) The phase separation underlying the pyrenoid-based microalgal Rubisco supercharger. *Nat. Commun.* 9, 5076
19. Freeman Rosenzweig, E.S. *et al.* (2017) The eukaryotic CO_2-concentrating organelle is liquid-like and exhibits dynamic reorganization. *Cell* 171, 148–162
20. Engel, B.D. *et al.* (2015) Native architecture of the *Chlamydomonas* chloroplast revealed by in situ cryo-electron tomography. *Elife* 4, e04889
21. Mukherjee, A. and Moroney, J.V. (2019) How protein-protein interactions contribute to pyrenoid formation in *Chlamydomonas*. *J. Exp. Bot.* 70, 5033–5035
22. Blanco-Rivero, A. *et al.* (2012) Phosphorylation controls the localization and activation of the lumenal carbonic anhydrase in *Chlamydomonas reinhardtii*. *PLoS ONE* 7, e49063
23. Sinetova, M.A. *et al.* (2012) Identification and functional role of the carbonic anhydrase CAH3 in thylakoid membranes of pyrenoid of *Chlamydomonas reinhardtii*. *Biochim. Biophys. Acta* 1817, 1248–1255
24. Itakura, A.K. *et al.* (2019) A Rubisco-binding protein is required for normal pyrenoid number and starch sheath morphology in *Chlamydomonas reinhardtii*. *Proc. Natl. Acad. Sci. U. S. A.* 116, 18445–18454
25. Toyokawa, C. *et al.* (2020) Pyrenoid starch sheath is required for LCIB localization and the CO_2-concentrating mechanism in green algae. *Plant Physiol.* 182, 1883–1893
26. Fei, C. *et al.* (2022) Modelling the pyrenoid-based CO_2-concentrating mechanism provides insights into its operating principles and a roadmap for its engineering into crops. *Nat. Plants* 8, 583–595
27. Mackinder, L.C.M. *et al.* (2016) A repeat protein links Rubisco to form the eukaryotic carbon-concentrating organelle. *Proc. Natl. Acad. Sci. U. S. A.* 113, 5958–5963
28. Ang, W.S.L. *et al.* (2023) The stickers and spacers of Rubiscondensation: assembling the centrepiece of biophysical CO_2-concentrating mechanisms. *J. Exp. Bot.* 74, 612–626
29. He, S. *et al.* (2020) The structural basis of Rubisco phase separation in the pyrenoid. *Nat. Plants* 6, 1480–1490
30. Wunder, T. and Mueller-Cajar, O. (2020) Biomolecular condensates in photosynthesis and metabolism. *Curr. Opin. Plant Biol.* 58, 1–7
31. He, G. *et al.* (2023) Phase-separating pyrenoid proteins form complexes in the dilute phase. *Commun. Biol.* 6, 19
32. Payne-Dwyer, A. *et al.* (2024) Predicting Rubisco-linker condensation from titration in the dilute phase. *Phys. Rev. Lett.* 132, 218401
33. Zhan, Y. *et al.* (2018) Pyrenoid functions revealed by proteomics in *Chlamydomonas reinhardtii*. *PLoS ONE* 13, e0185039
34. Lau, C.S. *et al.* (2023) A phase-separated CO_2-fixing pyrenoid proteome determined by TurboID in *Chlamydomonas reinhardtii*. *Plant Cell* 35, 3260–3279
35. Wang, L. *et al.* (2023) A chloroplast protein atlas reveals punctate structures and spatial organization of biosynthetic pathways. *Cell* 186, 3499–3518
36. Meyer, M.T. *et al.* (2020) Assembly of the algal CO_2-fixing organelle, the pyrenoid, is guided by a Rubisco-binding motif. *Sci. Adv.* 6, eabd2408
37. Waheeda, K. *et al.* (2023) Molecular mechanism of Rubisco activase: dynamic assembly and Rubisco remodeling. *Front. Mol. Biosci.* 10, 1125922
38. Bracher, A. *et al.* (2015) Degradation of potent Rubisco inhibitor by selective sugar phosphatase. *Nat. Plants* 1, 14002
39. Li, P. *et al.* (2012) Phase transitions in the assembly of multivalent signalling proteins. *Nature* 483, 336–340
40. Mitrea, D.M. and Kriwacki, R.W. (2016) Phase separation in biology; functional organization of a higher order. *Cell Commun. Signal.* 14, 1
41. Adler, L. *et al.* (2023) The role of BST4 in the pyrenoid of *Chlamydomonas reinhardtii*. *bioRxiv*, Published online November 17, 2023. https://doi.org/10.1101/2023.06.15.545204
42. Fauser, F. *et al.* (2022) Systematic characterization of gene function in the photosynthetic alga *Chlamydomonas reinhardtii*. *Nat. Genet.* 54, 705–714
43. Hennacy, J.H. *et al.* (2024) SAGA1 and MITH1 produce matrix-traversing membranes in the CO_2-fixing pyrenoid. *Nat. Plants*, Published online November 15, 2024. https://doi.org/10.1038/s41477-024-01847-0
44. Han, J. *et al.* (2017) The multifaceted role of SNARE proteins in membrane function. *Front. Physiol.* 8, 5
45. Villarejo, A. *et al.* (1996) The induction of the CO_2 concentrating mechanism in a starch-less mutant of *Chlamydomonas reinhardtii*. *Physiol. Plant.* 98, 799–802
46. Mangan, N.M. *et al.* (2016) pH determines the energetic efficiency of the cyanobacterial CO_2 concentrating mechanism. *Proc. Natl. Acad. Sci. U. S. A.* 113, E5354–E5362
47. Yamano, T. *et al.* (2022) CO_2-dependent migration and relocation of LCIB, a pyrenoid-peripheral protein in *Chlamydomonas reinhardtii*. *Plant Physiol.* 188, 1081–1094
48. Shimamura, D. *et al.* (2023) A pyrenoid-localized protein SAGA1 is necessary for Ca^{2+}-binding protein CAS-dependent expression of nuclear genes encoding inorganic carbon transporters in *Chlamydomonas reinhardtii*. *Photosynth. Res.* 156, 181–192
49. Xiang, Y. *et al.* (2001) The Cia5 gene controls formation of the carbon concentrating mechanism in *Chlamydomonas reinhardtii*. *Proc. Natl. Acad. Sci. U. S. A.* 98, 5341–5346

50. Fang, W. *et al.* (2012) Transcriptome-wide changes in *Chlamydomonas reinhardtii* gene expression regulated by carbon dioxide and the CO_2-concentrating mechanism regulator CIA5/CCM1. *Plant Cell* 24, 1876–1893
51. Brueggeman, A.J. *et al.* (2012) Activation of the carbon concentrating mechanism by CO_2 deprivation coincides with massive transcriptional restructuring in *Chlamydomonas reinhardtii*. *Plant Cell* 24, 1860–1875
52. Im, C.S. and Grossman, A.R. (2002) Identification and regulation of high light-induced genes in *Chlamydomonas reinhardtii*. *Plant J.* 30, 301–313
53. Gao, H. *et al.* (2015) Expression activation and functional analysis of HLA3, a putative inorganic carbon transporter in *Chlamydomonas reinhardtii*. *Plant J.* 82, 1–11
54. Duanmu, D. *et al.* (2009) Knockdown of limiting-CO_2-induced gene HLA3 decreases $HCO3^-$ transport and photosynthetic C_i affinity in *Chlamydomonas reinhardtii*. *Proc. Natl. Acad. Sci. U. S. A.* 106, 5990–5995
55. Yamano, T. *et al.* (2015) Characterization of cooperative bicarbonate uptake into chloroplast stroma in the green alga *Chlamydomonas reinhardtii*. *Proc. Natl. Acad. Sci. U. S. A.* 112, 7315–7320
56. Thever, M.D. and Saier, M.H. (2009) Bioinformatic characterization of p-type ATPases encoded within the fully sequenced genomes of 26 eukaryotes. *J. Membr. Biol.* 229, 115–130
57. Wang, Y. and Spalding, M.H. (2014) Acclimation to very low CO_2: contribution of limiting CO_2 inducible proteins, LCIB and LCIA, to inorganic carbon uptake in *Chlamydomonas reinhardtii*. *Plant Physiol.* 166, 2040–2050
58. Förster, B. *et al.* (2023) The *Chlamydomonas reinhardtii* chloroplast envelope protein LCIA transports bicarbonate in planta. *J. Exp. Bot.* 74, 3651–3666
59. Owji, A.P. *et al.* (2021) Structure and function of the bestrophin family of calcium-activated chloride channels. *Channels* 15, 604–623
60. Kono, A. and Spalding, M.H. (2020) LCI1, a *Chlamydomonas reinhardtii* plasma membrane protein, functions in active CO_2 uptake under low CO_2. *Plant J.* 102, 1127–1141
61. Kasili, R.W. *et al.* (2023) LCIB functions as a carbonic anhydrase: evidence from yeast and *Arabidopsis* carbonic anhydrase knockout mutants. *Photosynth. Res.* 156, 193–204
62. Kono, A. *et al.* (2020) Structure and function of LCI1: a plasma membrane CO_2 channel in the *Chlamydomonas* CO_2 concentrating mechanism. *Plant J.* 102, 1107–1126
63. Spalding, M.H. *et al.* (1983) Reduced inorganic transport in a CO_2-requiring mutant of *Chlamydomonas reinhardtii*. *Plant Physiol.* 73, 273–276
64. Burlacot, A. and Peltier, G. (2023) Energy crosstalk between photosynthesis and the algal CO_2-concentraing mechanisms. *Trends Plant Sci.* 28, 795–807
65. Allen, J.F. (2003) Cyclic, pseudocyclic and noncyclic photophosphorylation: new links in the chain. *Trends Plant Sci.* 8, 15–19
66. Lucker, B. and Kramer, D.M. (2013) Regulation of cyclic electron flow in *Chlamydomonas reinhardtii* under fluctuating carbon availability. *Photosynth. Res.* 117, 449–459
67. Sültemeyer, D.F. *et al.* (1987) Effect of dissolved inorganic carbon on oxygen evolution and uptake by *Chlamydomonas reinhardtii* suspensions adapted to ambient and CO_2-enriched air. *Photosynth. Res.* 12, 25–33
68. Burlacot, A. *et al.* (2022) Alternative photosynthesis pathways drive the algal CO_2-concentrating mechanism. *Nature* 605, 366–371
69. Findinier, J. *et al.* (2024) Dramatic changes in mitochondrial subcellular location and morphology accompany activation of the CO_2 concentrating mechanism. *bioRxiv*, Published online March 27, 2024. https://doi.org/10.1101/2024.03.25.586705
70. Águila Ruiz-Sola, M. *et al.* (2023) Light-independent regulation of algal photoprotection by CO_2 availability. *Nat. Commun.* 14, 1977
71. Wilson, S. *et al.* (2023) Overexpression of LHCSR and PsbS enhance light tolerance in *Chlamydomonas reinhardtii*. *J. Photochem. Photobiol. B* 244, 112718
72. Brangwynne, C.P. *et al.* (2009) Germline P granules are liquid droplets that localize by controlled dissolution/condensation. *Science* 324, 1729–1732
73. Etibor, T.A. *et al.* (2021) Liquid biomolecular condensates and viral lifecycles: Review and perspectives. *Viruses* 13, 366
74. Emenecker, R.J. *et al.* (2021) Biological phase separation and biomolecular condensates in plants. *Annu. Rev. Plant Biol.* 72, 17–46
75. Dignon, G.L. *et al.* (2020) Biomolecular phase separation: from molecular driving forces to macroscopic properties. *Annu. Rev. Phys. Chem.* 71, 53–75
76. Ginell, G.M. and Holehouse, A.S. (2023) An introduction to the stickers-and-spacers framework as applied to biomolecular condensates. *Methods Mol. Biol.* 2563, 95–116
77. Holehouse, A.S. and Pappu, R.V. (2018) Functional implications of intracellular phase transitions. *Biochemistry* 57, 2415–2423
78. Guillén-Boixet, J. *et al.* (2020) RNA-induced conformational switching and clustering of G3BP drive stress granule assembly by condensation. *Cell* 181, 346–361
79. Amin, M.A. *et al.* (2008) Depletion of nucleophosmin leads to distortion of nucleolar and nuclear structures in HeLa cells. *Biochem. J.* 415, 345–351
80. Banani, S.F. *et al.* (2017) Biomolecular condensates: organizers of cellular biochemistry. *Nat. Rev. Mol. Cell Biol.* 18, 285–298
81. McSwiggen, D.T. *et al.* (2019) Evaluating phase separation in live cells: diagnosis, caveats, and functional consequences. *Genes Dev.* 33, 1619–1634
82. Musacchio, A. (2022) On the role of phase separation in the biogenesis of membraneless compartments. *EMBO J.* 41, e109952